

LETTERS

Pressure-induced H bonding: Neutron diffraction study of brucite, $\text{Mg}(\text{OD})_2$, to 9.3 GPa

JOHN B. PARISE, KURT LEINENWEBER, DONALD J. WEIDNER, KEMIN TAN

CHIPR and Department of Earth and Space Sciences, State University of New York, Stony Brook, New York 11794-2100, U.S.A.

ROBERT B. VON DREELE

LANSCE, Los Alamos National Laboratory, Los Alamos, New Mexico 87545, U.S.A.

ABSTRACT

The structure of deuterated brucite has been refined using Rietveld analysis of neutron powder diffraction data collected in an opposed-anvil high-pressure (Paris-Edinburgh) cell from 0.4 to 9 GPa. On the basis of bond length changes obtained from the structure refinements, H bonding between the octahedral layers becomes more significant as the unit cell contracts. The *c* axis is approximately two times as compressible as the *a* axis in this pressure range, and the compression along *c* is largely taken up by a 13% reduction of the interlayer spacing. The O-D bond length, on the other hand, remains nearly constant or increases slightly over the pressure range. The position of D was modeled as a threefold split site of one-third occupancy each. The splitting between these sites increases with pressure, as does the O-D···O angle, whereas the interlayer D···O distance decreases, indicating a strengthening of the H bonding between the layers.

INTRODUCTION

Knowledge of the pressure dependence of H bonding in materials is of importance in understanding their stability and crystal chemistry. Brucite, a simple crystalline hydroxide, is an end-member for the hydrous minerals that are hosts for H_2O in the crust and mantle of the Earth. Recently Leinenweber and Weidner (1993) have shown that the brucite structure is stabilized to its melting point at high pressure, a result suggesting that a strengthening of the H bond at high pressure is sufficient to overcome the entropy gain upon dehydration. Several authors have presented arguments for and against pressure-induced H bonding, based upon spectroscopic (Kruger et al., 1989; Duffy, 1993) and theoretical studies (D'Arco et al., 1993; Sherman, 1991). The geophysical implications of stabilizing more complex OH-bearing phases (Gasparik, 1990; Finger et al., 1991; Liu, 1987; Pacalo and Parise, 1992) in the Earth's interior have also been reviewed by Thompson (1992) and Tyburczy et al. (1991).

Despite recent theoretical calculations indicating no strengthening of H bonding at high pressure (Sherman, 1991) we decided to test this possibility experimentally. Powder neutron diffraction is the most powerful technique for the determination of structure for hydrogenous materials at high pressure. Since the introduction of the

Paris-Edinburgh cell (Nelmes et al., 1993) the prospects for gaining new insights into changes in H bonding with pressure have greatly improved. This cell provides pressures in excess of 10 GPa—a usable range at least four times greater than previously attainable—with a large sample volume and no Bragg peaks from the sample holder. Its installation at spallation sources provides for superior data of the type required for Rietveld structural refinement (Larson and Von Dreele, 1986; Nelmes et al., 1993).

The crystal structure of brucite (Zigan and Rothbauer, 1967; Hyde and Andersson, 1989) is trigonal, space group $P\bar{3}m1$. It is composed of hexagonally close-packed layers of O, in which half the octahedral sites are occupied, forming sheets of MgO_6 octahedra (Fig. 1). Each O atom is hydrogenated with the O-H bond directed along the threefold axis toward the vacant tetrahedral site in the adjacent layer; the O-H bond lengths are 0.995 Å, and the separation of H atoms between layers is 2 Å. The spacing between H and the trio of second-neighbor O atoms, which is denoted D···O in Figure 1, is 2.458 Å at ambient pressure.

EXPERIMENTAL

Brucite was synthesized by hydrothermal treatment of high-purity MgO in the presence of D_2O (Sigma, 99.8%

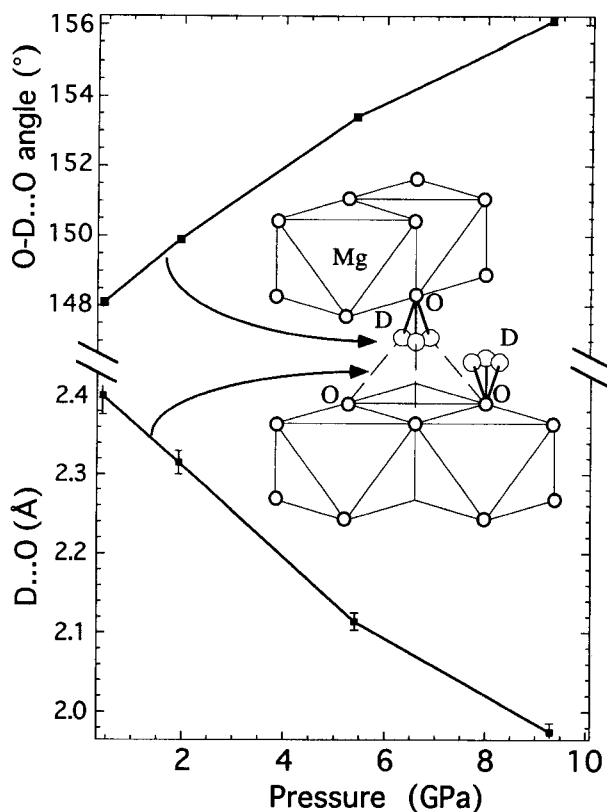


Fig. 1. Variation in the O-D...O angle and the interlayer O...D distance as a function of pressure found in this study. A polyhedral representation of the structure of deuterated brucite, $\text{Mg}(\text{OD})_2$, is shown. The polyhedra are Mg-centered, and the D sites (shown as circles) are $\frac{1}{3}$ occupied and at the $6i$ position.

D) in welded Au capsules held at 200 MPa and 600 °C for 1 week in cold-seal vessels. The product was confirmed as brucite by X-ray powder diffraction. In addition, the material was found to be well crystallized. In contrast, a second sample of deuterated brucite synthesized under autogenous conditions (200 °C) showed significant peak broadening, with peaks about three times as broad as those of the high-temperature sample. The high-temperature sample was used for neutron powder diffraction study.

A 152-mg sample of $\text{Mg}(\text{OD})_2$ was mixed with 27 mg of NaCl, which was used as an internal pressure calibrant. This was slurried with fluorinert FC-70 (3M company) and loaded into a Paris-Edinburgh high-pressure cell with tungsten carbide anvils (Nelmes et al., 1993) having a 100-mm³ spherical sample volume. Metal gaskets (Ti-Zr) were used to contain the sample, and oil pressure in the ram was raised using a hand pump. The data were taken at 300 K on the high intensity neutron powder diffractometer (HIPD) at the Manuel Lujan, Jr., Neutron Scattering Center (LANSCE) at the Los Alamos National Laboratory. The HIPD has a flight path of 9.0 m and a resolution $\Delta d/d$ of $5-7 \times 10^{-3}$. Data were collected in two detector banks, centered at $\pm 90^\circ 2\theta$, for about 12 h

at average proton currents of 65 μA on the spallation source. Portions of the diffraction data collected in the 90° data banks are shown in Figure 2.¹

The refinement was initiated using published data (Hyde and Andersson, 1989), with Mg at (0,0,0), O and D at $(\frac{1}{3}, \frac{2}{3}, z)$. Several cycles of least squares were used to adjust the unit cell, background, and peak width parameters (Larson and Von Dreele, 1986) before adjusting the structure model. For pressures up to 1.9 GPa there was no broadening greater than instrumental and no evidence of the particle-size broadening observed in a previous study of deuterated brucite (Partin et al., 1994). However, at 5.4 and 9.3 GPa peaks were broadened by factors of 2 and 5, respectively. This was presumed to be due to deviatoric stress and sample heterogeneities (Weidner et al., 1994). The values of the pressure-induced isotropic microstrain, as estimated from the σ_1 profile coefficient (Larson and Von Dreele, 1986), are 0.32, 0.62, and 1.12% for the data sets at 1.9, 5.4, and 9.2 GPa, respectively.

Three models for the structure were considered. Initially a model assuming isotropic thermal motion and all atoms on either the 3 or $\bar{3}$ axes was refined. A difference-Fourier map calculated from the data at 5.4 GPa clearly showed positive residual scattering around the site occupied by D. Further, models in which an anisotropic thermal parameter was refined for D resulted in the ratio U_{11}/U_{33} , increasing from 3 at 0.4 GPa to 10 at 5.4 GPa. The former ratio is in excellent agreement with that found in an earlier study by Zigan and Rothbauer (1967). Improvement to the overall fit of the isotropic model to observed data was obtained when D was moved from side $2d$ at $(\frac{1}{3}, \frac{2}{3}, z)$ to $6i$ at $(x, 2x, z)$, with occupation factor $\frac{1}{3}$. For example, the values for χ^2 for the 5.4 and 9.3 GPa data improved from 1.92 and 2.25 to 1.75 and 1.92, respectively. The values for R_{Bragg} for the 5.4 and 9.3 GPa data improved from 10 and 12% to 8 and 9%, respectively. The split-atom model was used for the analysis of the four data sets. In the final stages of the refinements, data from both the $+90^\circ$ and -90° banks were included. Refined parameters for the split-atom model are given in Table 1. The pressures were determined using the Decker (1971) equation of state for NaCl and the refined unit-cell parameters.

Following submission of this work, a redetermination of the room-pressure structure of portlandite, $\text{Ca}(\text{OH})_2$, which is isostructural with brucite, was published (Desgranges et al., 1993). This determination, like that of brucite before it (Zigan and Rothbauer, 1967), noted the unusually large U_{11}/U_{33} ratio. A split-site model proposed by Desgranges et al. (1993) for the H position is similar to that proposed by ourselves for the D position in brucite at high pressure.

¹ A copy of Fig. 2 may be obtained by ordering Document AM-94-549 from the Business Office, Mineralogical Society of America, 1130 Seventeenth Street NW, Suite 330, Washington, DC 20036, U.S.A. Please remit \$5.00 in advance for the microfiche.

TABLE 1. Refined atomic parameters* and selected interatomic distances (Å) and angles (°) for the split atom model of deuterated brucite, Mg(OD)₂

P (GPa)	0.4	1.9	5.4	9.3
a (Å)	3.1382(2)	3.1167(3)	3.0728(4)	3.0365(6)
c (Å)	4.713(1)	4.630(1)	4.496(1)	4.403(2)
U (Å ²)	40.20(1)	38.95(1)	36.77(1)	35.16(2)
z _O	0.214(3)	0.219(2)	0.229(2)	0.232(2)
U _{iso} (O)**	0.5(1)	0.7(1)	1.0(1)	1.0(1)
x _O	0.367(4)	0.373(3)	0.389(2)	0.402(2)
z _D	0.412(2)	0.417(2)	0.435(2)	0.449(2)
U _{iso} (D)**	1.7(4)	1.3(3)	1.2(3)	1.0(4)
F _{wp} †	4.28	3.77	3.98	3.90
R _p	3.01	2.70	2.68	2.83
χ ²	1.56	1.87	1.79	1.93
Mg-O × 6	2.074(6)	2.065(4)	2.052(4)	2.029(4)
Octa. thick.	2.02(1)	2.03(1)	2.06(1)	2.04(1)
Interlayer	2.70(2)	2.60(2)	2.44(2)	2.36(2)
O-Mg-O‡	98.3(4)	98.0(3)	97.0(2)	96.9(3)
⁶ⁱ e §	0.50	0.48	0.42	0.42
D ··· D	0.31(3)	0.37(2)	0.51(2)	0.63(2)

* Space group $P\bar{3}m1$, Mg at site 1a, (0,0,0); O atom at (1/3, 2/3, z). D moved from site 2d at (1/3, 2/3, z) to 6i at (x, 2x, z).

** Values × 10²; thermal parameters for Mg constrained to equal those for O.

† See Larson and Von Dreele (1986) for definitions of the discrepancy indices.

‡ The remaining angles between cis-O atoms are -(O-Mg-O) values given; trans O atoms are at 180°.

§ Octahedral strain (Zhao et al., 1993);

$$|^{6i}e| = \sqrt{\sum |e_i|^2} = \sqrt{\sum x_i^2 - (X_i - B - X_j)} \quad \text{for } i \neq j.$$

|| Distance in ångströms between split sites.

RESULTS AND DISCUSSION

The linear compressibility of the c axis was determined to be about two times that of the a axis, from the four data points in this study ($\beta_a = 0.0036$, $\beta_c = 0.0072$ GPa⁻¹). Fei and Mao (in preparation), in a diamond-anvil cell compression study with X-ray diffraction, found in contrast that the c axis was about five times as compressible as the a axis, for 15 data points between 1 and 14 GPa. The difference between the two measurements may be due to the different diffraction geometries, combined with nonhydrostatic stresses in either or both experiments. Acoustic velocity measurements at ambient conditions would be desirable to obtain axial compressibilities free of nonhydrostatic stress effects.

The bulk modulus of brucite from these measurements was determined to be 47(5) GPa, from the least-squares fit of the four data points to a second-order Birch-Murnaghan equation of state, which assumes $K' = 4.7$. For comparison, Fei and Mao (in preparation) obtained a value of 54.3(1.5) GPa and $K' = 4.7$ from a third-order Birch-Murnaghan equation of state fit to 35 data points between 2.5 and 33 GPa.

The greatest changes are in the interlayer separating the Mg sheets (Fig. 1, Table 1); although the thickness of the MgO₆ octahedron is constant (Table 1), the projected (O-O) interlayer distance decreases by 13% over the pressure range studied. The Mg-O distance decreases monotonically, whereas the octahedral strain (Zhao et al., 1993) appears to saturate at the highest pressures. The strength

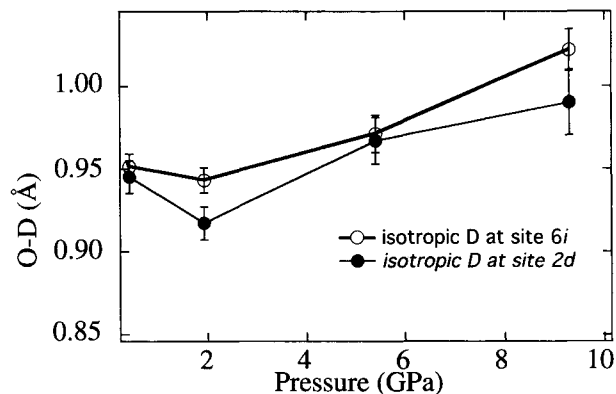


Fig. 3. Variation of the O-D distance with pressure for models in which (lower curve) D is fixed with full site occupancy at the site 2d (3m) and (upper curve) it is moved onto site 6i with site occupancy 1/3. Isotropic thermal parameters were used in both cases.

of the H bonding between layers increases with pressure. This is manifested in a decrease in the interlayer O ··· D distance and an increase in the O-D ··· O angle (Fig. 1). These changes are in the direction expected for an increase in the H bonding (Cotton and Wilkinson, 1980; Greenwood and Earnshaw, 1984). The movement of D to the 6i site can also be understood in this context. As the D ··· D distance between these partially occupied sites increases, the O-D ··· O angle decreases, and the D ··· O distance increases, forming stronger H bonds.

It is interesting to examine the present data in the context of spectroscopic and theoretical studies. Recent high-pressure infrared (Kruger et al., 1989) and Raman (Duffy, 1993) studies showed a decrease in the frequency of the O-H stretching mode, along with a broadening of the mode with pressure. In addition, a new Raman peak appeared at about 14 GPa, which was attributed to a previously unknown structural phase transition (Duffy, 1993). The slight lengthening of the O-D distance (Fig. 3), in contrast to the shrinkage of D ··· O, complements the spectroscopic observation of a decrease in the O-H stretching frequency. The frequency decrease is due to a decrease of the O-H stretching force constant, which alone does not require bond lengthening (Desgranges et al., 1993); however, our results suggest that some O-D bond lengthening occurs with pressurization. These data combined are strong evidence of an increase in the H ··· O or D ··· O attraction at high pressures, resulting in local distortion of the brucite structure. This could also result in an energetic stabilization of brucite at high pressure.

The finding that at higher pressure a considerable proportion of the D density occurs at three sites around the ideal D site is indicative of an additional feature of the H bonding that was not considered in previous theoretical studies (Sherman, 1991). The data indicate that off-axis motions of the D atoms may be part of the mechanism of H bonding in brucite. The absence of this consideration from the theory may account for the lack of enhancement of H bonding in the Hartree-Fock study of Sherman (1991).

The three off-axis D sites in the present model are randomly occupied within the resolution of the data, since no superstructure reflections appear in the diffraction patterns at any pressure studied. It is not obvious whether the three sites are a result of random static disorder or are due to anharmonic thermal vibrations between the three sites. It is possible that lower temperature or higher pressure could cause a superstructure ordering of each D atom into one of the three sites. Ordering of the H atoms, while maintaining the MgO-framework in the brucite structure, would require the removal of the threefold axis. The highest symmetry maximal nonisomorphic subgroup of $P\bar{3}m1$ consistent with these requirements is the space group $C2/m$. This is one possibility for the phase transition that was observed at 14 GPa in the Raman study of Duffy (1993) but which has not been directly observed in X-ray diffraction studies. A phase transition that mostly involves H ordering would not be expected to have an easily resolved X-ray signature.

Clearly, neutron diffraction data at higher pressures and lower temperatures would be desirable to elucidate the structure and bonding in brucite further and possibly to solve the phase transition observed in Raman spectra. In addition, theoretical calculations that allow for tilting of the O-H bonds away from the *c* axis would be useful in understanding the high-pressure behavior of this material.

ACKNOWLEDGMENTS

We gratefully acknowledge Donald Lindsley for his synthesis of high-purity MgO and for the use of high-pressure hydrothermal equipment for the synthesis of deuterated brucite. Support for this work includes funds from the NSF through grants DMR-9024249 and EAR-8917119. Research carried out in part at LANSCE, supported by the U.S. Department of Energy, Basic Energy Sciences Division, Division of Materials Science and Division of Chemical Sciences, Contract W-7405-ENG-36. CHiPR is an NSF-funded science and technology center; MPI contribution no. 108.

REFERENCES CITED

- Cotton, F.A., and Wilkinson, G. (1980) *Advanced inorganic chemistry: A comprehensive text*, p. 219–228. Wiley-Interscience, New York.
- D'Arco, P., Causa, M., Roetti, C., and Silvi, B. (1993) Periodic Hartree-Fock study of a weakly bonded layer structure: Brucite Mg(OH)₂. *Physical Review B*, 47, 3522–3529.
- Decker, D.L. (1971) High-pressure equation of state for NaCl, KCl and CsCl. *Journal of Applied Physics*, 42, 3239–3244.
- Desgranges, L., Grebille, D., Calvarin, G., Chevrier, G., Floquet, N., and Niepce, J.-C. (1993) Hydrogen thermal motion in calcium hydroxide: Ca(OH)₂. *Acta Crystallographica*, B49, 812–817.
- Duffy, T.S. (1993) A Raman spectroscopic study of a high-pressure phase transition in brucite. *Eos*, spring meeting, abstract m42B-8, p. 169.
- Finger, L.W., Hazen, R.M., and Prewitt, C.T. (1991) Crystal structures of Mg₁₂Si₄O₁₉(OH)₂ (phase B) and Mg₁₄Si₃O₂₄ (phase AnhB). *American Mineralogist*, 76, 1–7.
- Gasparik, T. (1990) Phase relations in the transition zone. *Journal of Geophysical Research*, 95, 15751–15769.
- Greenwood, N.N., and Earnshaw, A. (1984) *Chemistry of the elements*, p. 57–69. Pergamon, Oxford, England.
- Hyde, B.G., and Andersson, S. (1989) *Inorganic crystal structures*, p. 137–138. Wiley Interscience, New York.
- Kruger, M.B., Williams, Q., and Jeanloz, R. (1989) Vibrational spectra of Mg(OH)₂ and Ca(OH)₂ under pressure. *Journal of Chemical Physics*, 91, 5910–5915.
- Larson, A.C., and Von Dreele, R.B. (1986) GSAS: General structure analysis system manual. Los Alamos National Laboratory Report LAUR 86-748.
- Leinenweber, K., and Weidner, D.J. (1993) MgO solubilities in H₂O above the brucite dehydration temperature (abs.). *Eos*, 74, 16.
- Liu, L.-g. (1987) Effects of H₂O on the phase behavior of the forsterite-enstatite system at high pressures and temperatures and implications for the Earth. *Physics of the Earth and Planetary Interiors*, 49, 142–167.
- Nelmes, R.J., Loveday, J.S., Wilson, R.M., Besson, J.M., Pruzan, P., Klotz, S., and Hull, S. (1993) Neutron diffraction study of the structure of deuterated ice VIII to 10 GPa. *Physical Review Letters*, 71, 1192–1195.
- Pacalo, R.E., and Parise, J.B. (1992) Crystal structure of superhydrous B, a hydrous magnesium silicate synthesized at 1400 °C and 20 GPa. *American Mineralogist*, 77, 681–684.
- Partin, D., Brese, N., O'Keefe, M., and Von Dreele, R.B. (1994) Neutron diffraction study of brucite to 10 K. *Journal of Solid State Chemistry*, in press.
- Sherman, D.M. (1991) Hartree-Fock band structure, equation of state, and pressure-induced hydrogen bonding in brucite, Mg(OH)₂. *American Mineralogist*, 76, 1769–1772.
- Thompson, A.B. (1992) Water in the Earth's upper mantle. *Nature*, 358, 295–302.
- Tyburczy, J.A., Duffy, T.S., Ahrens, T.A., and Lange, M.A. (1991) Shock wave equation of state of serpentine to 150 GPa: Implications for the occurrence of water in the Earth's lower mantle. *Journal of Geophysical Research*, 96, 18011–18027.
- Weidner, D.J., Wang, Y., and Vaughan, M.T. (1994) Yield strength at high pressure and temperature. *Geophysical Review Letters*, in press.
- Zhao, Y., Weidner, D.J., Parise, J.B., and Cox, D.E. (1993) Thermal expansion and structural distortion of perovskite: Data for NaMgF₃ perovskite, part I. *Physics of the Earth and Planetary Interiors*, 76, 1–16.
- Zigan, F., and Rothbauer, R. (1967) Neutronenbeugungsmessungen am Brucit. *Neues Jahrbuch für Mineralogie Monatshefte*, 137–143.

MANUSCRIPT RECEIVED NOVEMBER 5, 1993

MANUSCRIPT ACCEPTED DECEMBER 7, 1993